VIP Molecular Machine Very Important Paper

How to cite:
International Edition: doi.org/10.1002/anie.202102838
German Edition: doi.org/10.1002/ange.202102838

A Light-Operated Molecular Cable Car for Gated Ion Transport

Chenxi Wang[+], Shunkang Wang[+], Huiting Yang, Yanxin Xiang, Xuebin Wang, Chunyan Bao, Linyong Zhu, He Tian, and Da-Hui Qu**

Dedicated to Professor Vincenzo Balzani on the occasion of his 85th birthday

Abstract: *Inspired by the nontrivial and controlled movements of molecular machines, we report an azobenzene-based molecular shuttle* ***PR2****, which can perform light-gated ion transport across lipid membranes. The amphiphilicity and membrane-spanning molecular length enable* ***PR2*** *to insert into the bilayer membrane and efficiently transport K^+ (EC_{50} = 4.1 μM) through the thermally driven stochastic shuttle motion of the crown ether ring along the axle. The significant difference in shuttling rate between trans-****PR2*** *and cis-****PR2*** *induced by molecular isomerization enables a light-gated ion transport, i.e., ON/OFF in situ regulation of transport activity and single-channel current. This work represents an example of using a photoswitchable molecular machine to realize gated ion transport, which demonstrates the value of molecular machines functioning in biomembranes.*

Ion transport across the lipid bilayer is a key physiological process of cells in regulating the pH value, maintaining osmotic balance and transmitting cellular signals, which is essential for the delicate operation of life.[1] Designing artificial molecules to simulate this process can improve the understanding of the working principle of natural ion transporters,[2] and have great potential applications in life science and materials science.[3]

To simulate the high selectivity and efficiency of ion transport by natural ion transporters, great efforts have been made to develop artificial carriers or channels.[4] Some of them focus on optimizing the structures of natural transporters,[5] while others are committed to creating new synthetic ion transporters such as tubular hosts,[6] helical foldamers,[7] heteropolymers,[8] rigid-rod oligomers[9] and molecular knots.[10] Recently, our group also reported that an artificial molecular shuttle acted like a cable car in a bilayer membrane for selective ion transport, i.e., passively transported K^+ ions based on the stochastic back-and-forth shuttling of a wheel along a thread.[11]

In addition to the ion selectivity and efficiency, the gated ion transport also plays an important role in nature. Channelrhodopsins (ChRs) are a class of representative light-gated cation channels.[12] They perform gated ion transport through photoinduced conformational transformation and play an important physiological role in nerve signal transduction. Chemical photoswitches are molecules that can rapidly and reversibly transform their conformations under light stimulation. Inspired by the working mechanism of ChRs, chemical photoswitches have been incorporated with protein channels to realize gated ion transport.[13] However, due to the lack of a synthetic architecture that can quickly respond to light in lipid bilayers, synthetic transporters showing light-gated ion transport are extremely rare.[14] Early designed photoresponsive surfactants are simply confined to changing the membrane permeability by conformational transformation.[15] To overcome this dilemma, it is necessary to design and synthesize novel light-gated ion transporters.

It is well known that rotaxane-type systems can control the shuttle process by photoinduced conformational transformation of the photoswitch moieties.[16–19] If this light-controlled shuttling can be incorporated into the rotaxane transporter operated by our reported shuttle mechanism,[11a] it will be possible to realize light-gated ion transport across lipid membranes. As illustrated in Scheme 1, an azobenzene-based molecular shuttle (**PR2**, Scheme 1a) was designed, which includes an azobenzene-modified amphiphilic thread (**PT2**) with two secondary ammonium ions as the terminal stations for the shuttle and a wheel (**RCE**) consisting of a K^+ selective receptor, i.e., a benzo[18]crown-6 (B18C6) ring. The space length between the two ammonium stations of **PT2** is approximately 3.43 nm (calculated according to the Corey-Pauling-Koltun (CPK) model, Figure S1), which is comparable to the hydrophobic thickness of a typical phospholipid bilayer and enables the stable membrane-spanning arrangement of the rotaxane.[20] We envision that when the azobenzene moiety is in the *trans*-form, the ring can freely shuttle between the two secondary ammonium stations in the membrane, which results in efficient ion transport (Scheme 1b). After irradiation with 365 nm light, the photoisomerization of the azobenzene moiety from the *trans*- to the *cis*-form slows down or even prevents ring shuttling, which causes the light-gated behavior for ion transport. Therefore, the

[*] C. Wang,[+] S. Wang,[+] H. Yang, Y. Xiang, X. Wang, Prof. C. Bao, Prof. L. Zhu, Prof. H. Tian, Prof. D.-H. Qu
Key Laboratory for Advanced Materials and Joint International Research Laboratory of Precision Chemistry and Molecular Engineering
Feringa Nobel Prize Scientist Joint Research Center
Frontiers Science Center for Materiobiology and Dynamic Chemistry
Institute of Fine Chemicals, School of Chemistry and Molecular Engineering
East China University of Science and Technology
Shanghai 200237 (China)
E-mail: baochunyan@ecust.edu.cn
dahui_qu@ecust.edu.cn

[+] These authors contributed equally to this work.

Supporting information and the ORCID identification number(s) for the author(s) of this article can be found under: https://doi.org/10.1002/anie.202102838.

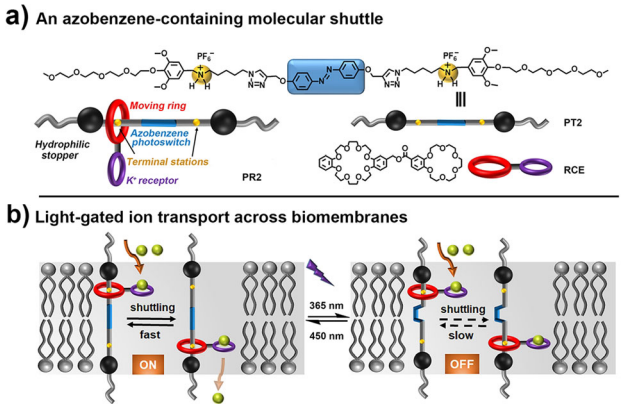

Scheme 1. a) Molecular structure of molecular shuttle **PR2** and b) proposed mechanism for light-gated ion transport across lipid bilayers.

integration of a light-responsive molecular machine with biological/biomimetic membranes will operate ion transport in a controllable and reproducible manner.

PR2 was prepared by a typical "threading followed by stopping" strategy (Schemes S1–S4). The interlocked structure can be verified by comparing the partial ^{1}H NMR spectra in CD_3CN with thread **PT2** and ring **RCE**. As shown in Figure 1 a, the appearance of complexed and noncomplexed thread protons, i.e., H_c, H_d, and H_e, indicates that the ring stays at one of the ammonium stations on the NMR time scale. It also shows that there is the *cis*-isomer of **PR2** (*cis*-**PR2**) in CD_3CN even without irradiation, and the *trans*-isomer can be totally converted into *cis*-isomer upon 365 nm UV irradiation. The photoconversion is further confirmed by the evolution of absorption, which shows reversible switches between *trans*- and *cis*-isomers (Figure 1 b, Figure S2). To investigate the isomerization effect on the shuttling rate, NMR exchange spectroscopy (2D-EXSY, Figure S3, S4 and Table S1) was performed, where $CDCl_3$ was used as the solvent because its hydrophobic environment is closer to the phospholipid bilayer. After data processing, the shuttling rate k of *trans*-**PR2** is 0.214 Hz as calculated by the exchange rates; however, no obvious exchange signal was detected when **PR2** was transferred into the *cis*-form upon 365 nm irradiation. The reversible isomerization and controllable shuttle motion of **PR2** provide the premise for gated ion transport across lipid bilayers.

To verify whether **PR2** can insert into lipid bilayers to perform ion transport, as in our previous molecular cable car, dynamic light scattering (DLS) analysis was first performed. Unlike the surfactant Triton X-100, which decomposes large unilamellar lipid vesicles (LUVs), the addition of **PR2** only slightly broadens the particle size distribution and does not break the membrane integrity (Figure S5). Differential scanning calorimetry (DSC) was used to evaluate the ability of compounds to incorporate liposomes, since it can monitor the domain information of the lipid membrane. The results show that the addition of **PR2** obviously alters the endothermal phase behavior of the membrane in the temperature range of 10–40 °C (Figure S6), which indicates the insertion of **PR2** in the lipid bilayers instead of only surface adsorption.[8,21] This

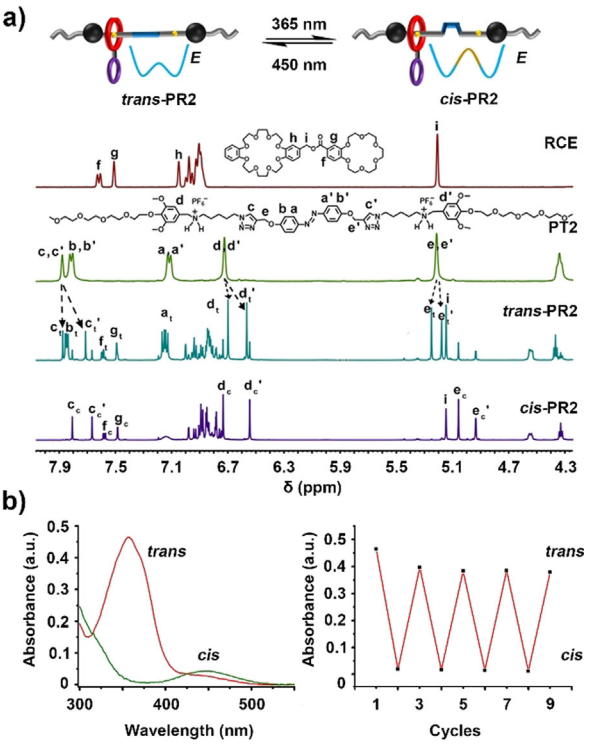

Figure 1. a) Partial ^{1}H NMR spectra (600 MHz) of the ring **RCE**, thread **PT2** and rotaxane **PR2** before and after 365 nm irradiation (2 min, 10 mW cm^{-2}) in CD_3CN at 1.0×10^{-2} M. Subscript "t" and "c" indicate the peaks assigned to *trans*- and *cis*-isomers, respectively. b) Reversible photoswitching of **PR2** (25.0 μM) in CH_3CN monitored by UV/Vis spectroscopy. The detection wavelength in the right panel is 360 nm.

conclusion can be further confirmed by the remaining characteristic absorption peak of **PR2** in LUVs after removing the extravehicular compounds by column purification (Figure S7). A patch clamp technique on planar lipid bilayer membranes (BLMs) was employed to record single-channel current traces. The regular square-like signals with considerably long opening times and the ohmic I–V profile confirm that **PR2** transports ions as fast as a stable channel or pore across the bilayer membrane (Figure 2, Figure S8). The conductance value was approximately 19 pS, which is close to that of gramicidin A (23.2 pS), which indicates the efficient transport of ions.[22]

An 8-hydroxy-1,3,6-pyrenetrisulfonate (HPTS) fluorescence-based LUVs assay was performed to explore the transport activity of **PR2**.[11a] As illustrated in Figure 3 a, a pH gradient was applied to a solution of HPTS-encapsulated LUVs (LUVs⊃HPTS) by addition of KOH (i.e., $\Delta pH = 0.8$) in the extravesicular buffer; then the addition of transporters induced the collapse of the pH gradient via a H^+ efflux or OH^- influx, which led to the change in the ratio of fluorescence intensity at 510 nm (I_{450}/I_{405}) of HPTS trapped inside the vesicles. *Trans*-**PR2** shows concentration-dependent transport activity (Figure 3 b) and reveals an EC_{50} (the effective concentration required for 50 % activity in 450 s) value of 4.1 μM (12.4 mol % relative to lipid, Table S2), which was significantly greater than that of subunits **PT2** (Figure S9) and comparable to our reported rotaxane transporter with

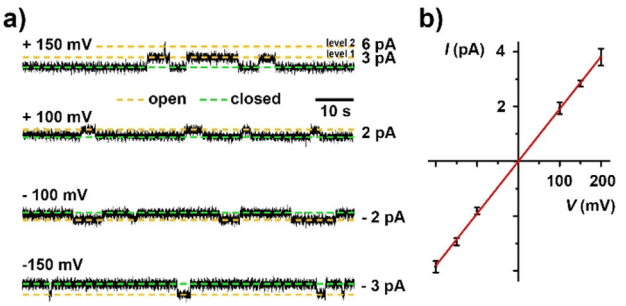

Figure 2. a) Representative current recording and b) linear *I*–*V* plots of **PR2** (2.5 μM) at various holding potentials in a symmetrical 1 M KCl solution; "open" means the opening of current signal; "closed" means the current signal is zero; "level 1" means the signals from a single channel; and "level 2" means the signals from two channels.

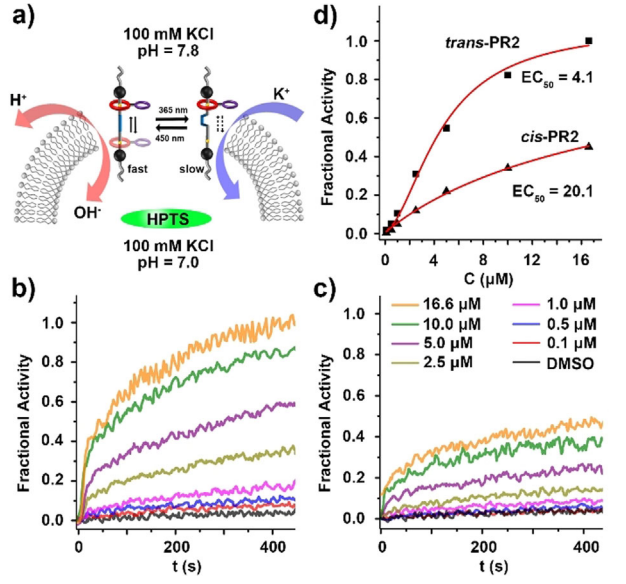

Figure 3. a) Schematic illustration of the pH-sensitive LUVs⊃HPTS assay. b,c) Ion transport activities of *trans*-**PR2** (b) and *cis*-**PR2** (c) at 0.1–16.6 μM. d) Comparison of the concentration–activity curves. The red lines are the fitted curves from Hill equation (see Supporting Information, section 9).

two stations, i.e., 6.7 μM.[11a] Further plotting the observed rate constant k_{obs} against the concentrations (Figure S10), the linear correlation indicates the unimolecular active structure of **PR2** for ion transport. Considering the matching molecular length of **PR2** (3.43 nm hydrophobic spacer) with the thickness of the insulator regime of lipid bilayers, we can conclude that **PR2** inserts and spans the entire bilayer to transport ions. To explore the action of ionophore B18C6, both cation and anion selectivity were explored and recorded by varying ions outside the liposomes. **PR2** exhibited obvious cation selectivity and the transport activity follows the order of $K^+ > Cs^+ > Na^+ \geq Rb^+ > Li^+$ (Figure S11,12), which is inconsistent with the energy penalty of ion dehydration,[23] indicating that the ion recognition of B18C6 causes the K^+ selectivity. It suggests that either the K^+/OH^- symport or the K^+/H^+ antiport plays the key role for the fluorescence change of HPTS. Then, a selective H^+ transporter, carbonyl cyanide-4-(trifluoromethoxy)phenylhydrazone (FCCP), was added as the cotransporter (Figure S13). The increased fractional activity from 0.5 to 0.8 indicates that the transport of K^+ is faster than that of H^+. To prove that ion transport of **PR2** does not originate from the disruption of the membrane, a HPTS leakage experiment and a preincorporated LUVs assay were performed (Figure S14,15). The low leakage and a comparable transport activity (1 mol% to lipids) verify that the transmembrane activity originates from the insertion of **PR2** rather than membrane destabilization. After UV light irradiation, *cis*-**PR2** exhibits much lower transmembrane activity (Figure 3c,d) with an EC_{50} value of 20.1 μM (theoretical value from Hill equation, 60.9 mol% relative to lipid). The decrease in transport activity of *cis*-**PR2** is consistent with the suggested shuttling-based transport mechanism; i.e., the limited shuttle motion of the *cis*-isomer reduces the transport activity. This is notably different from membrane-active molecules containing azobenzene, which exhibit an improved ion transport ability after the *cis*-isomerization due to the increased membrane disruption.[15]

The in situ light regulation of **PR2** in the membrane was also performed by alternating irradiation between 365 nm UV and 450 nm visible light. The UV/Vis absorption analysis confirms the successful isomer transformation of **PR2** in lipid bilayers (Figure S7, Figure S16). The isomerization does not result in the removal of molecules from lipids and the isomers have good dark stability in the lipid membrane. Firstly, the pH-gradient LUVs⊃HPTS assay was used to explore the in situ optical switch of transport activity (Figure S17). To obtain a longer observation period, activity tracking began with the addition of *cis*-**PR2** with low transport activity. As illustrated in Figure 4a, the fractional activity shows light-gated ON/OFF by alternating 450 nm and 365 nm illumination. This is one of the few studies to observe in situ light-gated transmembrane activity using a liposome experiment.[24] Then, single-channel conductance experiments on BLMs were performed to exploit the light-gated behavior (Figure S18). As illustrated in Figure 4b (Figure S19), reversible switching between open and closed states was observed for the isomers embedded in a lipid membrane. After the addition of *cis*-**PR2**, no current signal was detected for a long time; however, regular square-like signals appeared after 450 nm visible light irradiation. If the patch was irradiated with 365 nm UV light again, the channel current almost switched back to silent. After more than 20 traces were counted, the opening probability P_0 of *trans*-**PR2** was much higher than that of *cis*-**PR2**. All these results support our hypothesis that molecular machine **PR2** can insert into the membrane to transport ions like a cable car, and the conformational transformation of azobenzene can reversibly regulate the shuttling-rate to realize light-gated ion transport as demanded.

In summary, an azobenzene-based molecular shuttle **PR2** was synthesized and used as a vehicle to develop a light-gated ion transport function in lipid bilayer membranes. Due to the geometrical transformations of the azobenzene moiety, shuttle motions of **PR2** can be controlled by light. Significant differences in shuttling motion between *trans*-**PR2** and *cis*-**PR2** result in light-gated K^+ transport across lipid mem-

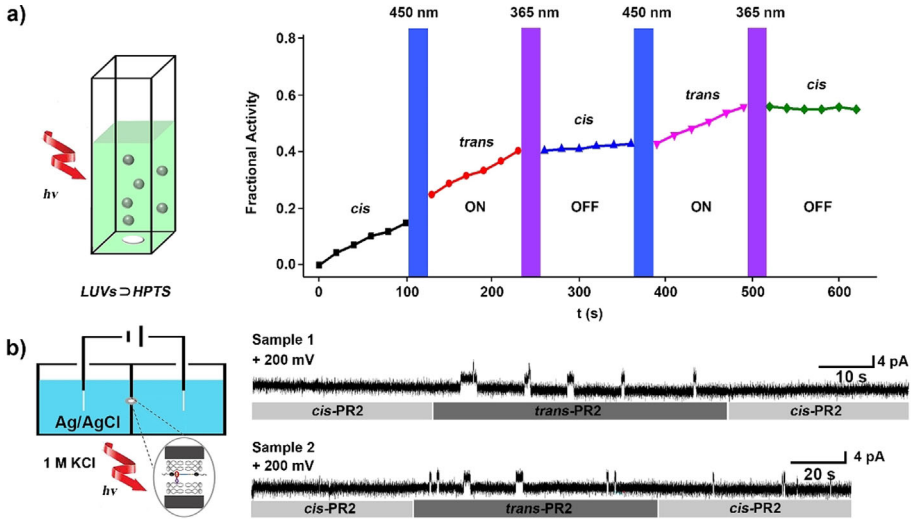

Figure 4. a) Light-regulated fractional activity analysis of **PR2** (10.0 μM) on LUVs⊃HPTS. b) Two representative current traces in patch clamp experiments for the in situ photoswitching of **PR2** (2.5 μM) on BLMs; the holding potential is 200 mV. Alternating 365 nm UV and 450 nm visible light triggers the switching behavior.

branes, such as the ON/OFF regulation of the transport activity on LUVs and the OPEN/CLOSED current recordings on BLMs. This study represents a case of light-gated ion transport in lipid bilayers controlled by synthetic photoresponsive molecular machines, which provides an important step towards creating biomimetic artificial systems with signalling feedback and opening a new direction for future therapeutic applications.

Acknowledgements

This work was supported by the National Key Research and Development Project (2019YFA0110500), NSFC/China (22025503, 21790361 and 21871084), Shanghai Municipal Science and Technology Major Project (grant 2018SHZDZX03), the Fundamental Research Funds for the Central Universities, the Programme of Introducing Talents of Discipline to Universities (grant B16017), Program of Shanghai Academic/Technology Research Leader (19XD1421100). We thank Dr. Chengxi Zhao for his help in the calculation of molecular structure optimization. We thank the Research Centre of Analysis and Test of East China University of Science and Technology for the help with the characterization.

Conflict of interest

The authors declare no conflict of interest.

Keywords: artificial ion transport · host–guest system · light-gating · molecular machine · rotaxanes

[1] a) R. MacKinnon, *Angew. Chem. Int. Ed.* **2004**, *43*, 4265 – 4277; *Angew. Chem.* **2004**, *116*, 4363 – 4376; b) M. A. Zaydman, J. R. Silva, J. Cui, *Chem. Rev.* **2012**, *112*, 6319 – 6333; c) J. T. Davis, O. Okunola, R. Quesada, *Chem. Soc. Rev.* **2010**, *39*, 3843 – 3862.

[2] C. Maffeo, S. Bhattacharya, J. Yoo, D. Wells, A. Aksimentiev, *Chem. Rev.* **2012**, *112*, 6250 – 6284.

[3] a) N. Busschaert, S.-H. Park, K.-H. Baek, Y. P. Choi, J. Park, E. N. W. Howe, J. R. Hiscock, L. E. Karagiannidis, I. Marques, V. Félix, W. Namkung, J. L. Sessler, P. A. Gale, I. Shin, *Nat. Chem.* **2017**, *9*, 667 – 675; b) F. Mohammad, J. C. Stewart, S. Ott, K. Chlebikova, J. Y. Chua, T.-W. Koh, J. Ho, A. Claridge-Chang, *Nat. Methods* **2017**, *14*, 271 – 274.

[4] a) X. Wu, E. N. W. Howe, P. A. Gale, *Acc. Chem. Res.* **2018**, *51*, 1870 – 1879; b) A. L. Sisson, M. R. Shah, S. Bhosale, S. Matile, *Chem. Soc. Rev.* **2006**, *35*, 1269 – 1286; c) S.-P. Zheng, L.-B. Huang, Z. Sun, M. Barboiu, *Angew. Chem. Int. Ed.* **2021**, *60*, 566 – 597; *Angew. Chem.* **2021**, *133*, 574 – 606; d) D. S. Kim, J. L. Sessler, *Chem. Soc. Rev.* **2015**, *44*, 532 – 546.

[5] a) G. A. Woolley, A. S. I. Jaikaran, Z. Zhang, S. Peng, *J. Am. Chem. Soc.* **1995**, *117*, 4448 – 4454; b) J. L. Sessler, L. R. Eller, W.-S. Cho, S. Nicolaou, A. Aguilar, J. T. Lee, V. M. Lynch, D. J. Magda, *Angew. Chem. Int. Ed.* **2005**, *44*, 5989 – 5592; *Angew. Chem.* **2005**, *117*, 6143 – 6146.

[6] W. Si, P. Xin, Z.-T. Li, J.-L. Hou, *Acc. Chem. Res.* **2015**, *48*, 1612 – 1619.

[7] a) X. Wei, G. Zhang, Y. Shen, Y. Zhong, R. Liu, N. Yang, F. Y. Al-Mkhaizim, M. A. Kline, L. He, M. Li, Z. L. Lu, Z. Shao, B. Gong, *J. Am. Chem. Soc.* **2016**, *138*, 2749 – 2754; b) F. Chen, J. Shen, N. Li, A. Roy, R. Ye, C. Ren, H. Zeng, *Angew. Chem. Int. Ed.* **2020**, *59*, 1440 – 1444; *Angew. Chem.* **2020**, *132*, 1456 – 1460.

[8] T. Jiang, A. Hall, M. Eres, Z. Hemmatian, B. Qiao, Y. Zhou, Z. Ruan, A. D. Couse, W. T. Heller, H. Huang, M. O. de la Cruz, M. Rolandi, T. Xu, *Nature* **2020**, *577*, 216 – 220.

[9] S. Chen, Y. Zhao, C. Bao, Y. Zhou, C. Wang, Q. Lin, L. Zhu, *Chem. Commun.* **2018**, *54*, 1249 – 1252.

[10] D. P. August, S. Borsley, S. L. Cockroft, F. della Sala, D. A. Leigh, S. J. Webb, *J. Am. Chem. Soc.* **2020**, *142*, 18859 – 18865.

[11] a) S. Chen, Y. Wang, T. Nie, C. Bao, C. Wang, T. Xu, Q. Lin, D. H. Qu, X. Gong, Y. Yang, L. Zhu, H. Tian, *J. Am. Chem. Soc.* **2018**, *140*, 17992 – 17998; b) A. Credi, *Angew. Chem. Int. Ed.* **2019**, *58*, 4108 – 4110; *Angew. Chem.* **2019**, *131*, 4152 – 4155.

[12] G. Nagel, D. Ollig, M. Fuhrmann, S. Kateriya, A. M. Musti, E. Bamberg, P. Hegemann, *Science* **2002**, *296*, 2395 – 2398.

[13] a) A. Kocer, M. Walko, W. Meijberg, B. L. Feringa, *Science* **2005**, *309*, 755 – 758; b) N. L. Mutter, J. Volarić, W. Szymanski, B. L. Feringa, G. Maglia, *J. Am. Chem. Soc.* **2019**, *141*, 14356 – 14363; c) H. Janovjak, S. Szobota, C. Wyart, D. Trauner, E. Y. Isacoff, *Nat. Neurosci.* **2010**, *13*, 1027 – 1032; d) T. Fehrentz, M. Schönberger, D. Trauner, *Angew. Chem. Int. Ed.* **2011**, *50*, 12156 – 12182; *Angew. Chem.* **2011**, *123*, 12362 – 12390.

[14] a) T. Liu, C. Bao, H. Wang, Y. Lin, H. Jia, L. Zhu, *Chem. Commun.* **2013**, *49*, 10311 – 10314; b) P. V. Jog, M. S. Gin, *Org. Lett.* **2008**, *10*, 3693 – 3696; c) Y. Zhou, Y. Chen, P.-P. Zhu, W. Si, J.-L. Hou, Y. Liu, *Chem. Commun.* **2017**, *53*, 3681 – 3684.

[15] a) Y. Lei, J. Hurst, *Langmuir* **1999**, *15*, 3424 – 3429; b) R. A. Moss, W. Jiang, *Langmuir* **1995**, *11*, 4217 – 4221.
[16] a) T. Ogoshi, D. Kotera, S. Fa, S. Nishida, T. Kakuta, T. Yamagishi, A. M. Brouwer, *Chem. Commun.* **2020**, *56*, 10871 – 10874; b) G. Tabacchi, S. Silvi, M. Venturi, A. Credi, E. Fois, *ChemPhysChem* **2016**, *17*, 1913 – 1919; c) S. Corra, M. Curcio, S. Silvi, A. Credi, *Adv. Mater.* **2020**, *32*, 1906064.
[17] a) M. Baroncini, M. Canton, L. Casimiro, S. Corra, J. Groppi, M. L. Rosa, S. Silvi, A. Credi, *Eur. J. Inorg. Chem.* **2018**, 4589 – 4603; b) H. Murakami, A. Kawabuchi, K. Ketoo, M. Kunitake, N. Nakashima, *J. Am. Chem. Soc.* **1997**, *119*, 7605 – 7606.
[18] a) R. Ballardini, V. Balzani, A. Credi, M. T. Gandolfi, M. Venturi, *Acc. Chem. Res.* **2001**, *34*, 445 – 455; b) V. Balzani, A. Credi, S. Silvi, M. Venturi, *Chem. Soc. Rev.* **2006**, *35*, 1135 – 1149; c) V. Balzani, A. Credi, M. Venturi, *Chem. Soc. Rev.* **2009**, *38*, 1542 – 1550.
[19] a) W. Abraham, K. Buck, M. Orda-Zgadzaj, S. Schmidt-Schäffer, U. Grummt, *Chem. Commun.* **2007**, 3094 – 3096; b) A. Credi, S. Silvi, M. Venturi, *Top. Curr. Chem.* **2014**, *354*, 1 – 34.
[20] L. J. Lis, M. Mcalister, N. Fuller, R. P. Rand, V. A. J. B. J. Parsegian, *Biophys. J.* **1982**, *37*, 657 – 665.
[21] M. Fidorra, L. Duelund, C. Leidy, A. C. Simonsen, L. A. Bagatolli, *Biophys. J.* **2006**, *90*, 4437 – 4451.
[22] C. Ren, J. Shen, H. Zeng, *J. Am. Chem. Soc.* **2017**, *139*, 12338 – 12341.
[23] a) G. Eisenman, R. Horn, *J. Membr. Biol.* **1983**, *76*, 197 – 225; b) G. Lamoureux, B. Roux, *J. Phys. Chem. B* **2006**, *110*, 3308 – 3322.
[24] a) A. Kerckhoffs, M. J. Langton, *Chem. Sci.* **2020**, *11*, 6325 – 6331; b) R. F. Khairutdinov, J. K. Hurst, *Langmuir* **2004**, *20*, 1781 – 1785.

Manuscript received: February 25, 2021
Revised manuscript received: March 30, 2021
Accepted manuscript online: April 11, 2021
Version of record online: ■■ ■■, ■■■■

Communications

Molecular Machine

C. Wang, S. Wang, H. Yang, Y. Xiang, X. Wang, C. Bao,* L. Zhu, H. Tian, D.-H. Qu* ——— ■■■■–■■■■

A Light-Operated Molecular Cable Car for Gated Ion Transport

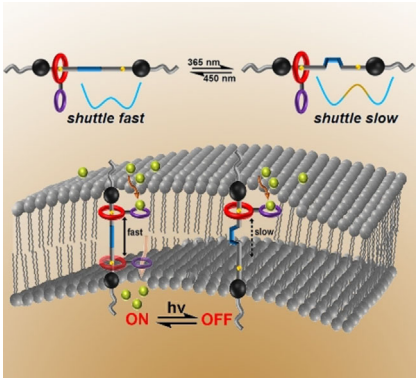

Inspired by natural rhodopsin, an azobenzene-based molecular rotaxane was designed to insert into lipid membranes for the regulation of ion transport. Based on the shuttle transport mechanism, the significant difference in shuttling rate between *trans*- and *cis*-isomer caused by molecular isomerization facilitates light-gated ion transport.